Available online at www.sciencedirect.com
ScienceDirect
Catalysis Today 126 (2007) 394–399
CATALYSIS TODAY
www.elsevier.com/locate/cattod

# Rapid synthesis of $La_{0.7}Sr_{0.3}MnO_{3+\lambda}$ catalysts by microwave irradiation process

Rui Ran, Duan Weng *, Xiaodong Wu, Jun Fan, Liang Qing

*Key Laboratory for Advanced Materials of Ministry of Education, Department of Materials Science & Engineering, Tsinghua University, Beijing 100084, PR China*

Available online 20 July 2007

**Abstract**

Microwave irradiation processing (MIP) was considered as a potential method to synthesize perovskite-type oxides rapidly, cleanly and energy-efficiently. In this paper, $La_{0.7}Sr_{0.3}MnO_{3+\lambda}$, a kind of promising catalyst for automobile exhaust purification, was successfully prepared by MIP in not more than 5 min. The sol–gel method was also used for comparison. All the samples were evaluated by catalytic activity tests in the simulated exhaust and characterized by XRD, BET, TEM and XRF analyses. The results showed that the integrated perovskite-type phase and uniform particle size were obtained in the microwave-treated samples. And those ones exhibited a better oxidation activity under slightly oxygen-rich condition than that by sol–gel method, which may be related to more A-site cation vacancies and larger bulk oxygen content generated in MIP. Possible formation mechanism of perovskites in MIP was also discussed.


*Keywords:* Perovskite; Microwave irradiation; Catalytic activity

## 1. Introduction

The conception of microwave sintering was first reported by Tinga [1] in 1960s and has been intensively investigated since the mid of 1970s by Badot and Berteand [2]. In the late 1980s, microwave was brought into the field of materials science and was gradually developed as a novel rapid sintering technique to be used in various high performance ceramics and alloys [3], such as $ZrO_2$, $Si_3N_4$, SiC, $BaTiO_3$, $SrTiO_3$, PZT, $TiO_2$, $Al_2O_3$–TiC, etc. After then, the microwave irradiation process (MIP), one of the novel processes which evolved from microwave sintering, was widely applied in inorganic/organic synthesis [4–7], food drying [8], microwave-induced catalysis [9] and plasma chemistry [10]. With its rapid development in recent decades, MIP has obtained a growing interest, especially in materials synthesis research [7].

The advantages of MIP has been summarized as below [4,7]: (i) rapid reaction velocity; (ii) uniform heating; (iii) clean and energy efficient. The microwave preparations have been reported to be operated usually in domestic microwave ovens at ca. 2.45 GHz and with a maximum output power not less than 1 kW. The microwave energy can be absorbed by dielectric materials and transformed into heat energy directly via the polarization and dielectric loss in the interior of materials [4]. According to the electromagnitism, the heating rate of the experimental materials can be formulated as:

$$\frac{\Delta T}{t} = \frac{0.566 \times 10^{-10} \varepsilon''_{\text{eff}} f E^2}{\rho C_P} \quad (1)$$

where $\varepsilon''_{\text{eff}}$ is the effective dielectric loss; $f$ the microwave frequency; $E$ the intension of electric field; $\rho$ the mass density of the sample, and $C_P$ is the isotonic specific heat [4]. In this case, the energy utilization efficiency can easily reach 80–90%, which is much higher than the conventional route [2,3]. However, the essential nature of the interaction between microwave and reactants during material synthesis is somewhat unclear and speculative.

Perovskite-type oxides (PTOs, general formula $ABO_3$) are technologically important. They are widely used in solid oxide fuel cells (SOFCs) [11], magnetic properties [12], and catalysis applications [13–18]. Especially, PTOs has a lot of advantages for catalyst design: the lattice sites A and B can be accessed differently by substitution, and almost 90% of all metallic

* Corresponding author. Tel.: +86 10 62772726; fax: +86 10 62772726.
*E-mail address:* duanweng@tsinghua.edu.cn (D. Weng).

0920-5861/$ – see front matter © 2007 Elsevier B.V. All rights reserved.
doi:10.1016/j.cattod.2007.06.008

elements can be incorporated into a perovskite structure, even in unusual oxidation states [19]. As the development of nanoscience has occurred to us significantly, multifarious soft-chemical and self-assembly methods have been brought into the preparation of PTOs in the passed few decades, to increasingly precise control of the variables affecting physicochemical properties [14–20]. However, most of them need both high calcination temperature (>700 °C) and long time (>3 h) for pretreatment or sintering. MIP is suggested to be the most potential method to reduce the disadvantages above.

During the past years, a lot of PTOs, such as $GaAlO_3$, $LaCrO_3$, $LaCoO_3$ and $LaNiO_3$, etc., have been reported to be synthesized by MIP for their ferroelectricity, superconductivity, high-temperature ionic conductivity, or a variety of magnetic ordering, etc. [20–22]. It was reported that smaller grain size and more rapid lattice diffusion would be formed in microwave route than other wet chemical processes [24], which might enhance the lattice oxygen mobility in catalysis process. Nevertheless, none of them focused on the catalytic activity of PTOs catalysts. Since the lanthanum manganate are one of the most catalytically interesting perovskites with oxygen excessive nonstoichiometry, in this work, we mainly dealt with the microstructure of Sr-doped $LaMnO_3$ perovskite-type oxides synthesized by MIP and their three-way catalytic activity under slightly oxygen-rich condition. Possible formation mechanisms were also discussed.

## 2. Experimental

### 2.1. Preparation of catalysts

For the preparation of $La_{0.7}Sr_{0.3}MnO_{3+\lambda}$ catalysts, a stoichiometric mixture of respective nitrates $La(NO_3)_3$ (Aldrich), $Sr(NO_3)_2$ (Aldrich), and $Mn(NO_3)_2$ (Aldrich) were dissolved in 20 ml deionized water according to the molar ratio of La:Sr:Mn = 0.7:0.3:1. The solution was exposed to microwaves in ambient atmosphere and irradiated with microwaves in a simple domestic microwave oven (Glanze WD800 (BL23), China) operating at 2.45 GHz with a maximum power of 800 W for 3 min, 3 min 15 s, 3 min 30 s, 4 min and 5 min, respectively, which were referred to as M3, M31, M32, M4 and M5, respectively. During this time water in the solution got evaporated, and companied with nitrogen oxides ($NO_x$) generating, the nitrates got decomposed. The resulting oxides reacted and formed $La_{0.7}Sr_{0.3}MnO_{3+\lambda}$ peroveskites. The temperature in this process was measured with an infrared pyrometer. For comparison, a sol–gel process was performed with citric acid as the complexing agent to get the sample SGC. The aqueous solution was mixed by using the corresponding nitrates with the same molar ratio. Citric acid was added to the aqueous solution as the complexing species, whose mole summation equalled to that of metal ions of $La^{3+}$, $Sr^{2+}$ and $Mn^{2+}$. Appropriate glycol was added as the dispersant followed by evaporation and peptization. The sol was heated at 100 °C until a spongy dark gel remained. Then the gel was submitted to decomposition at 300 °C for 1 h and calcination at 750 °C for 3 h by 10 °C $min^{-1}$.

### 2.2. Characterization of catalysts

The prepared powders were characterized using X-ray diffraction (XRD) for phase identification. The XRD was conducted on a Japan Science D/max-RB diffractometer employing Cu Kα radiation (λ = 1.5418 Å, DS = 1°). The X-ray tube was operated at 40 kV and 120 mA. The X-ray powder diffractograms were recorded at 0.02° intervals in the range $20^\circ \leq 2\theta \leq 80^\circ$ with 2 s count accumulation per step. Specific surface areas were calculated by the Brunauer–Emmett–Teller (BET) method from the $N_2$ adsorption isotherms, recorded at liquid nitrogen temperature on a micromeritics apparatus model NOVO-4000. Prior to the adsorption measurements, samples were out-gassed at 200 °C for 4 h. Transmission electron microscopy (TEM, JEM 1200EX) was also carried out to observe the morphology of the powders and estimate the particle size. Elemental analysis of samples was performed by means of X-ray fluorescence analysis (XRF).

### 2.3. Activity test

0.5 g powder catalyst sample was mixed homogeneously with coarse quartz particles with a total volume of 3 ml. The mixture was loaded in a quartz reaction tube with the diameter of 25 mm. The three-way catalytic activity was evaluated in a tube microreactor by passing a gas mixture simulated to exhaust from gasoline engine. The simulated exhaust contained a mixture of $O_2$ (1.5%), CO (1.5%), $CO_2$ (12%), $C_3H_8$ ($1.05 \times 10^{-3}$), NO (0.05%) and $N_2$ (balance). The stoichiometry number, $S$, used to identify the redox characteristic of the feed streams and related to the $A/F$ ratio of the engine exhaust gas, was defined as follows:

$$S = \frac{2O_2 + NO}{CO + H_2 + 10C_3H_8} \quad (2)$$

The above values of reactant components corresponded to $S = 1.22$, which was in the oxygen-rich condition. The concentrations of CO, $C_3H_8$ and NO were determined on-line by a five-component analyzer (Siemens, German). For the light-off experiments, the reactor was heated from 200 to 650 °C in the flow stream at a gas space velocity (GSV) of 50,000 $h^{-1}$ and a total gas flow rate of 2500 ml $min^{-1}$.

## 3. Result

### 3.1. Structural properties

The XRD patterns for the samples treated in microwave field for 3 min, 3 min 15 s, 3 min 30 s, 4 min and 5 min are shown in Fig. 1. It is shown that, the sample mainly consists of $Sr(NO_3)_2$, $LaMnO_{3+\lambda}$ and some amorphous structure when treated for 3 min. Successively, it can be estimated from intensified peaks that better crystallization occurs efficiently with the treating time increasing. And after a longer time than 3 min, the XRD patterns of the samples agree well with those of an orthorhombic perovskite structure (space group *Pbnm*), with only a few weak peaks of the impurities. It is, therefore, implied

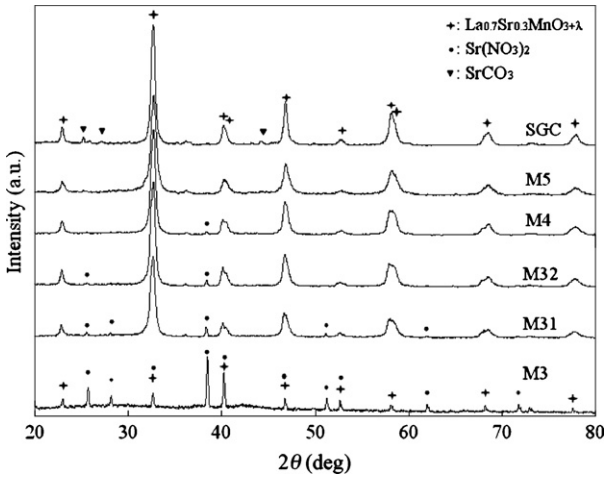


Fig. 1. XRD patterns of the samples by different methods.

that strontium has dissolved into the lattice of $LaMnO_{3+\lambda}$ and the PTOs $La_{0.7}Sr_{0.3}MnO_{3+\lambda}$ can be successfully synthesized by MIP during a short time.

According to the results above, it can be presumed that the microwave reactions involved in the formation of PTOs are as follows:

$$\text{Aqueous solution of } [La(NO_3)_3 + Mn(NO_3)_2] \overset{\text{microwave}}{\longrightarrow} La_2O_3 + MnO_x + \text{water} + NO_x \quad (3)$$

$$La_2O_3 + MnO_x \overset{\text{microwave}}{\longrightarrow} LaMnO_{3+\lambda} \quad (4)$$

$$LaMnO_{3+\lambda} + Sr(NO_3)_2 \overset{\text{microwave}}{\longrightarrow} La_{0.7}Sr_{0.3}MnO_{3+\lambda} + NO_x \quad (5)$$

In this process, the initial decomposition of $La(NO_3)_2$ and $Mn(NO_3)_2$ occurrs firstly, when the solution is placed in the microwave field for a while (Eq. (3)). And $Mn^{2+}$ is readily oxidized to $Mn^{3+}$ or $Mn^{4+}$ in situ by the formation of reactive oxygen during the nitrate decomposition. Manganese oxide is available to absorber of microwaves. Consequently, the reaction between the resulting oxides (Eq. (4)) goes so fast by the polarization and dielectric loss that no lanthanum and manganese oxides can be detected in the sample M3. Nevertheless, since the decomposition temperature of $Sr(NO_3)_2$ is much higher than those of $La(NO_3)_2$ and $Mn(NO_3)_2$, $La_{0.7}Sr_{0.3}MnO_{3+\lambda}$ is finally formed by the decomposition of $Sr(NO_3)_2$ and incorporation of Sr into the perovskite lattice (Eq. (5)).

The XRD patterns of the samples sythesized by sol–gel method is also displayed in Fig. 1. Compared with the sample SCG, less peaks of the impurities appear in the diffraction pattern of the microwave-treated samples M4 and M5, since the strontium carbonate can be easily formed from the corresponding citrate by the ununiform heating in conventional sintering. Accordingly, it evidences that the use of microwave for calcinations has an advantage in terms of homogeneous insertion or dispersion of strontium in lanthanum manganate.

The temperature profile of the reactants for the $La_{0.7}Sr_{0.3}MnO_{3+\lambda}$ samples in MIP was measured and the result is shown in Fig. 2a. It costs only 3 min to reach a temperature as high as 800 °C, which is high enough to make the reactions (3)–(5) happen. Since the main reaction happened in the aqueous solution at the first 2 min, the temperature of the solution was less than its boiling point, which could not be detected by the infrared pyrometer. Such a rapid process can be attributed to the volumetric heating in microwave field and the exothermic nature of the reaction [22]. To clarify the nature of heating in this case, the heating behaviors of $MnO_2$ and $La_2O_3$ cited from ref. [23] are also displayed in Fig. 2b. Manganese oxide is a dielectric material which is a good absorber of microwaves. It plays an important role of the microwave-adsorbing material in this case, while lanthanum trioxide cannot be heated efficiently in microwave field. Energy is, therefore, absorbed directly by the bulk of the sample which contains manganese. Generally, microwave can penetrate into the interior of dielectric materials (Fig. 3), and the heat wave spreads from the inner to the outer, which is contrary to the traditional process [4]. Consequently, the center of the sample is rapidly heated, and uniform heating is achieved to form an integrated perovskite phase.

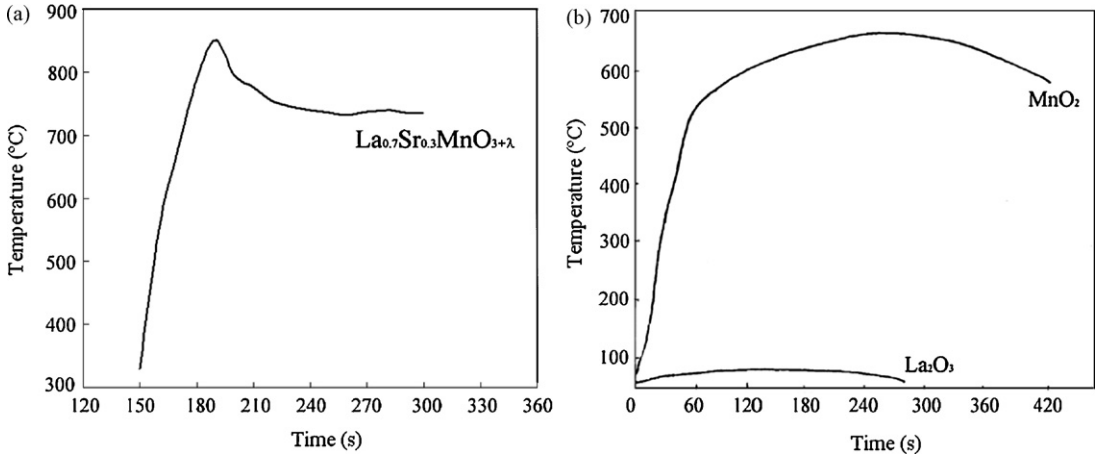


Fig. 2. Temperature profiles of (a) $La_{0.7}Sr_{0.3}MnO_{3+\lambda}$ and (b) $MnO_2$ and $La_2O_3$.

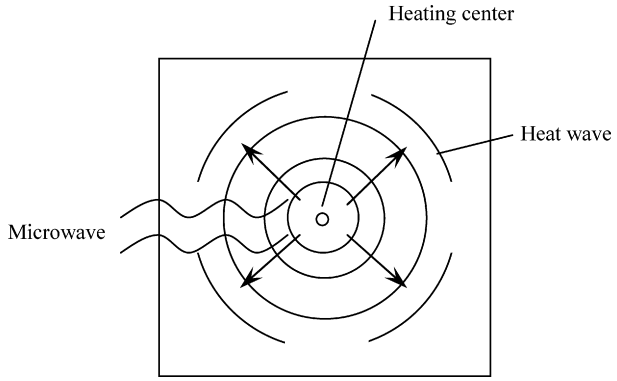


Fig. 3. The radiating process of heat wave induced by microwave irradiation.

### 3.2. Surface properties

The TEM micrographs in Fig. 4 confirm the structural characteristics of the samples. It can be seen that some amorphous structures exist in the sample M3, which correlates with the XRD result above. Correspondingly, the samples M31–M5, which were treated for a longer time, have much better crystallization and more uniform microstructure. The packed aggregates of M31–M5 comprise lots of nanoparticles with the size typically in the range of 20–50 nm. Furthermore, with increment of the treating time in microwave field, the crystallites of PTOs grow larger. The TEM micrograph of the powders synthesized by sol–gel method is also shown in Fig. 4. It is found that the particle size of M5 is more uniform than that of SCG, even if M5 has a little larger avarge particle size. So did M31–M4, which implies a more uniform heating condition was obtained in MIP than conventional calcining process.

The surface areas of these powders were measured by BET technique. The BET results show that the samples M5 and SGC retain a moderate and similar specific surface area of 15.9 and 16.3 $m^2\,g^{-1}$, respectively. Assuming spheroids particles, a mean value of diameter can be estimated by using Eq. (6) [25].

$$D = \frac{6}{\rho S} \tag{6}$$

where $D$ is the diameter in μm, $\rho$ the volumic mass in g $cm^{-3}$ and $S$ is the specific area in $m^2\,g^{-1}$. It can be calculated that their average particle size is 58.9 and 57.5 nm, respectively, which are close to the TEM observations.

### 3.3. Catalytic activity

The light-off performances of the microwave-treated sample M5 and sol–gel-synthesized sample SGC were tested under an oxygen-rich condition ($S = 1.22$). As seen in Fig. 5, in both cases the conversion of three pollutants CO, $C_3H_8$ and NO start at ca. 200, 300 and 400 °C, respectively. When $T < 300$ °C, the samples exhibit almost the same catalytic performance. At the medium temperature range (300–400 °C), the difference between the activities of two samples can be distinguished apparently. When $T > 400$ °C, the sample M5 has prominent better oxidation but worse reduction activities than SGC. On the other side, the oxygen concentration decreases sharply with the increases of HC and CO conversion rates over each sample. However, more oxygen remains for SGC after the reaction temperature reaching 370 °C, which may be related to the relative lower conversion of HC.

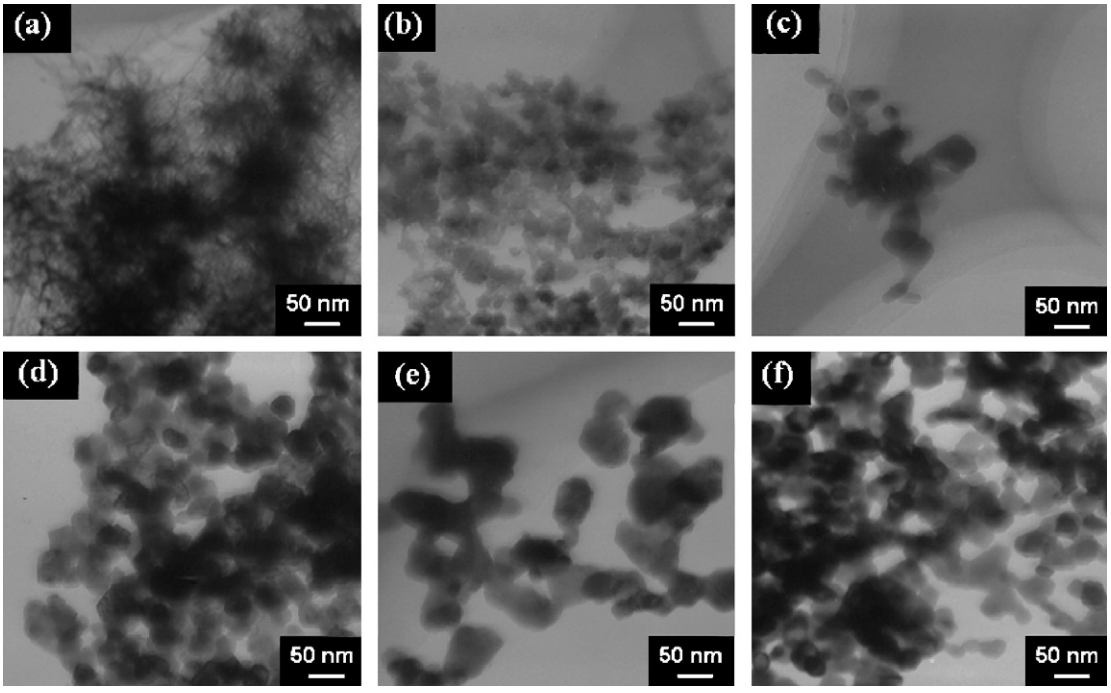


Fig. 4. TEM images of the samples (a) M3, (b) M31, (c) M32, (d) M4, (e) M5 and (f) SCG.

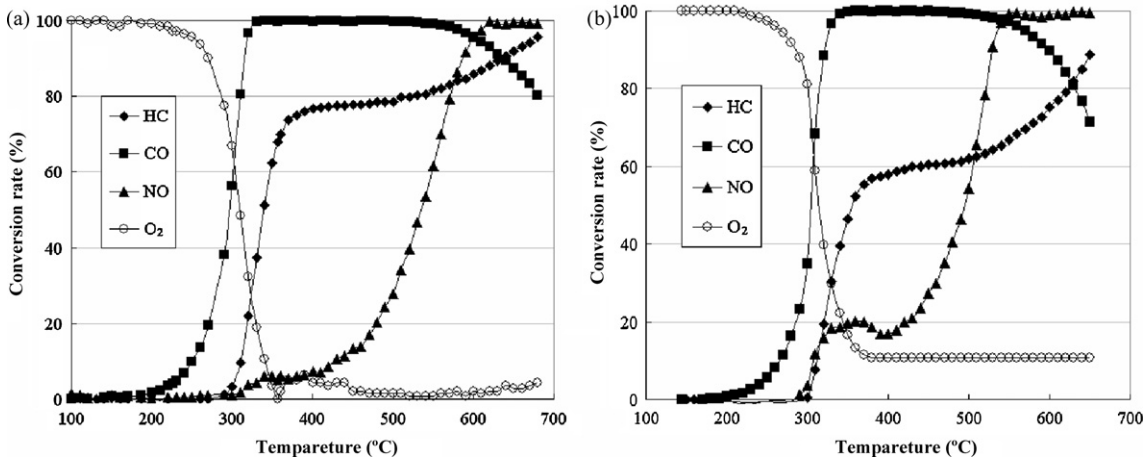


Fig. 5. Light-off curves of (a) M5 and (b) SGC.

As we know, there are two types of oxygen in perovskite-type oxides [26], and it is considered that the absorbed oxygen is the main reactive oxygen in perovskite at low-temperature, and then the lattice oxygen in the bulk becomes more and more dominant with the further increase of the temperature. According to this, it is suggested that the microwave irradiation treatment probably mainly lead different contents of lattice oxygen or structural defects.

For confirming the above speculation, XRF elemental analyses were taken to estimate the relative atom ratio of the elements. The precision of X-ray fluorescence analysis was inherently limited. In order to minimize the system error to some extent, SGC was considered here as the reference sample whose La:Sr:Mn:O ratio was set as 0.7:0.3:1:3 intentionally, although its cation and anion contents were most likely to be nonstoichiometry. It has been reported by Tanaka and Misono [27] that the $BO_3$ array in the perovskite structure forms a so stable network that the large A-site cations could be missing partially, thus, we calculated the stoichiometric factor of M5 by fixing the stoichiometric factor of Mn as 1. It is seen from Table 1 that the atom contents of La, Sr in M5 are actually lower than those of SCG. It confirms that more A-site cation vacancies are generated in the microwave treatment. Simultaneously, the ratio of oxygen in M5 is more nonstoichiometric. It shows that larger oxygen content has been attained in MIP, which may have some indirect effects on the state of lattice oxygen in the samples. Such a phenomenon is most likely attributed to their incomplete diffusion in such a rapid synthesis process. However, the mechanism of these changes remains unclear.

Table 1
The bulk composition of the samples determined by XRF

| Samples | La (at.%) | Sr (at.%) | Mn (at.%) | O (at.%) | Stoichiometric factor[b] |
|---|---|---|---|---|---|
| M5 | 12.923 | 5.7426 | 20.1811 | 61.1532 | $La_{0.64}Sr_{0.28}MnO_{3.03}$ |
| SGC[a] | 14 | 6 | 20 | 60 | $La_{0.7}Sr_{0.3}MnO_3$ |

[a] SGC was considered here as the reference sample whose La:Sr:Mn:O ratio was set as 0.7:0.3:1:3 intentionally.
[b] The stoichiometric factor of M5 was calculated by fixing the stoichiometric factor of Mn as 1.

## 4. Conclusions

A series of nanosized perovskite-type oxides $La_{0.7}Sr_{0.3}MnO_{3+\lambda}$ were successfully synthesized by microwave irradiation processing in a short time. The formation of $La_{0.7}Sr_{0.3}MnO_{3+\lambda}$ in MIP began with the decomposition of $La(NO_3)_2$ and $Mn(NO_3)_2$, and then the decomposition of $Sr(NO_3)_2$ companied with incorporation of Sr into the perovskite lattice. The better crystallization occurs efficiently with the increase of the treating time in microwave field. Compared with the sample SGC, the microwave-treated samples had the less impurities phase and more uniform particles. Meanwhile, a better oxidation activity were achieved in those samples, as well as more A-site cation vacancies and larger bulk oxygen content, which might be led by the incomplete diffusion in such a rapid synthesis process. It should be demonstrated that the microwave method (2.45 GHz) is a simple and efficient method which is probable to be utilized for the future preparation of perovskite-type catalysts.

## Acknowledgements

The authors would like to acknowledge Project 2004CB719503 and 2004AA649400 supported by the Ministry of Science and Technology, PR China. Moreover, we would also thank the Key Laboratory of Advance Materials, Tsinghua University for performing surface characterizations.

## References

[1] W.R. Tinga, W.A.G. Voss, Microwave Power Engineering, Academic Press, New York, 1968.
[2] A.J. Berteaud, J.C. Badet, Microwave Power 11 (1976) 315–320.
[3] P. Liu, H. Wang, X. Cheng, A. Shui, L. Zeng, China Ceram. 41 (4) (2005) 12–15.
[4] Q. Jin, Microwave Chemistry, China Science Press, Beijing, 1999.
[5] J. Motuzas, A. Julbe, R.D. Noble, C. Guizard, Z.J. Beresnevicius, D. Cot, Micropor. Mesopor. Mater. 80 (2005) 73–83.
[6] W.M. Dai, X. Wang, C. Ma, Tetrahedron 61 (2005) 6879–6885.
[7] K.J. Rao, B. Vaidhyanathan, M. Ganguli, P.A. Ramakrishnan, Chem. Mater. 11 (1999) 882–895.
[8] A. Altan, M. Maskan, Food Res. Int. 38 (2005) 787–796.

[9] G.D. Yadav, P.M. Bisht, Catal. Commun. 5 (2004) 259–263.
[10] B. Shokri, M. Ghorbanalilu, Phy. Lett. A 342 (2005) 341–346.
[11] Z. Shao, M.H. Sossina, Nature 431 (2004) 170.
[12] J.J. Blanco, M. Insausti, L. Lezama, J.P. Chapman, I. Gil de Muro, T. Rojo, J. Solid State Chem. 177 (2004) 2749–2755.
[13] X.D. Wu, L.H. Xu, D. Weng, Catal. Today 90 (2004) 199–206.
[14] N. Blangenois, M. Florea, P. Grange, Appl. Catal. A 263 (2004) 163–170.
[15] E. Krupicka, A. Reller, A. Weidenkaff, Crystal Eng. 5 (2002) 195–202.
[16] A.J. Zarur, J.Y. Ying, Nature 403 (2000) 65–67.
[17] Y. Mao, S. Banerjee, S. Wong, Chem. Commun. 3 (2003) 408–409.
[18] H. Kamiya, K. Gomi, Y. Iida, K. Tanaka, T. Yoshiyasu, T. Kakiuchi, J. Am. Ceram. Soc. 86 (12) (2003) 2011–2018.
[19] F. Haaβ, H. Fuess, Adv. Eng. Mater. 7 (2005) 899–913.
[20] M.P. Selvam, K. Rao, Adv. Mater. 12 (21) (2000) 1621.
[21] K.E. Gibbons, S.J. Blundell, A.I. Mihut, I. Gameson, P.P. Edwards, Y. Miyazaki, N.C. Hyatt, M.O. Jones, A. Porch, Chem. Commun. 1 (2000) 159–160.
[22] M.P. Selvam, K.J. Rao, J. Mater. Chem. 13 (2003) 596–601.
[23] A. Duan, Y. Dong, W. Tai, P. Liu, P. Hong, J. Yunnan Normal Univ. 18 (1) (1998) 78–81.
[24] H. Yan, X. Huang, Z. Lu, H. Hu, R. Xue, L. Chen, J. Power Sources 68 (1997) 530–532.
[25] L. Combemale, G. Caboche, D. Stuerga, D. Chaumont, Mater. Res. Bull. 40 (2005) 529–536.
[26] R.J. Voorhoeve, Advanced Materials in Catalysis, Academic Press, New York, 1977, p. 173.
[27] H. Tanaka, M. Misono, Curr. Opin. Solid State Mater. Sci. 5 (2001) 381.